Turk J Chem
34 (2010) , 935 – 943.

doi:10.3906/kim-1003-2

Synthesis and characterization of Ba/MCM-41

Emine KAYA[1], **Nuray OKTAR**[1,*], **Gürkan KARAKAŞ**[2], **Kırali MÜRTEZAOĞLU**[3]

[1] *Chemical Engineering Department, Gazi University, Maltepe, Ankara-TURKEY*

[2] *Chemical Engineering Department, METU, Ankara-TURKEY*

e-mail: nurayoktar@gazi.edu.tr

[3] *Chemical and Process Engineering Department, Bilecik University, Gülümbe, Bilecik-TURKEY*

Received 01.03.2010

Mesoporous Ba/MCM-41 type materials (Ba/MCM-41) with high Ba/Si molar ratios between 0.025 and 0.1 were synthesized by direct hydrothermal synthesis. The samples were characterized by XRD, nitrogen adsorption, TGA-DTA, FTIR, SEM-EDS, and TEM techniques. BET surface areas of samples with various Ba loadings were found between 722 and 931 m^2/g with 28 Å average pore size, which is consistent with the pore size of 30 Å for pure MCM-41 samples synthesized by the same procedure. The crystal structures of synthesized MCM-41 and Ba/MCM-41 were confirmed by XRD analysis. Among the investigated Ba/MCM-41 samples, the formation of barium oxide and barium nitrate species besides silicates was also observed in the high angle region XRD patterns.

Key Words: MCM-41, Ba, hydrothermal synthesis

Introduction

In 1992, a new family of silica based mesoporous materials known as MCM-41 was discovered by researchers at Mobil, and is the most widely studied mesoporous support material, possessing a hexagonal array of uniform mesopores with 15-100 Å pore size.[1,2] MCM-41 can be synthesized by a variety of synthesis methods,[3–7] and hydrothermal synthesis is the most applied method, basically utilizing a silica source, a mineralizing agent with structure-directing agent, and water as the solvent.[8]

Ordered mesoporous silicas are used as catalyst support by adding catalytic active sites to the silica walls or by deposition of active species on the inner surface of the materials.[9] Prior to the advantages stated above,

*Corresponding author

various metal containing MCM-41 catalysts were studied for a variety of reactions such as reforming, oxidation, polymerization, and NOx reduction.[10−16] NOx emissions from combustion sources cause acid rain, which is one of the most crucial environmental problems. The removal of NOx from emissions by reduction to N_2 and O_2 had been studied.[15−18] The reduction of NOx requires utilization of reducing agents such as ammonia and lower hydrocarbons, which is impractical for mobile sources. An alternative approach to reduction is the trapping and adsorption of NOx molecules in solid adsorbent. Ba-containing adsorbents were reported to be useful in NOx adsorption and have been studied extensively in the literature.[19−22] NOx adsorption was achieved in the studies performed by Cant without the need for extra oxygen according to the proposed model shown below:[19]

$$BaO + NO_2 \rightarrow BaO_2 + NO \quad (1)$$

$$BaO_2 + 2NO_2 \rightarrow Ba(NO_3)_2 \quad (2)$$

In the present study, Ba/MCM-41 materials with high surface areas were synthesized for different Ba/Si molar ratios varying between 0.025 and 0.1. Direct hydrothermal synthesis was applied, and characterization studies were performed to clarify the effect of metal addition on the molecular structure. The applied direct hydrothermal synthesis route was thought to enhance the uniform dispersion of the metal throughout the structure; hence materials with attractive properties for potential use in NOx storage were synthesized.

Experimental

Materials and synthesis method

Ba/MCM-41 materials were prepared by direct hydrothermal synthesis. In the hydrothermal synthesis of MCM-41 and Ba/MCM-41 materials, an aqueous solution of sodium silicate (Merck, containing 27 wt.% SiO_2), and hexadecyltrimethylammonium bromide (CTMABr, Merck 99% pure) was used as the silica source and surfactant respectively. MCM-41 was synthesized according to the procedure reported in the literature.[23] Surfactant solution was prepared by continuous mixing of 13.2 g of hexadecyltrimethylammonium bromide in 87 mL of deionized water at 30 °C. Sodium silicate solution was added to the surfactant solution dropwise, and the pH of the resulting mixture was adjusted to 11. The resulting gel was stirred for 1 h and then transferred into a Teflon-lined stainless steel autoclave for hydrothermal synthesis of MCM-41, at 120 °C, for 96 h. The precipitate was filtered, washed, and dried at 40 °C under vacuum, prior to calcination. Calcination was carried out in a tubular furnace, in a flow of dry air. During calcination, the furnace temperature was increased to 550 °C with a rate of 1 °C/min and kept at this temperature for 6 h and then cooled to room temperature by flowing air.

Ba incorporated MCM-41 materials with different Ba/Si molar ratios were prepared by a similar procedure with $Ba(NO_3)_2$ used as the barium source. In the synthesis of MCM-41, sodium silicate solution was added to the surfactant solution dropwise and then a corresponding amount of $Ba(NO_3)_2$ solution was slowly added to the resulting synthesis mixture. The pH of the mixture was adjusted to 11. The resulting gel was stirred for 1 h and then transferred into a Teflon-lined stainless steel autoclave for hydrothermal synthesis at 120 °C, for 96 h. The precipitate was filtered, washed, and dried at 40 °C under vacuum before calcination, which was carried out in a tubular furnace, in a flow of dry air. The samples were calcined with the same thermal procedure as the bare MCM-41 samples.

Characterization

The XRD patterns were collected using a Bruker/D8 Advance diffractometer with CuKα radiation ($\lambda = 1.5418$ Å), 2θ geometry, and a scintillation detector. Each diffraction pattern was recorded at a step of 0.01° and 1 s per step. All measurements were made at room temperature. The BET surface areas of the samples were measured by the N_2 adsorption method and pore distributions were determined by nitrogen adsorption desorption isotherms (Quantachrome Corporation, Autosorb-1-C/MS). Pore size distributions and pore diameter were calculated by the BJH method. Thermogravimetric analysis was performed in a TA INS. SDT Q600 device at a temperature between 25 and 800 °C, with a heating rate of 10 °C/min, under He flow. The IR spectra of samples were obtained by a Thermo Nicolet 8700 FT-IR spectrometer with a resolution of 4 cm^{-1}. The morphology of the adsorbents was determined by SEM-EDS (JEOL-JSN-811). TEM images were taken by using a TECNAI^{GM} G^2 F30 (100 kV).

Results and discussion

Mesostructured Ba/MCM-41 (Ba/Si: 0.025-0.1) type materials with high surface areas were prepared by a direct hydrothermal synthesis route. Calcined samples of bare MCM-41 and Ba/MCM-41 species were characterized by XRD, nitrogen adsorption, TGA-DTA, FTIR, SEM-EDS, and TEM analyses. The XRD patterns of bare MCM-41 and Ba/MCM-41 are shown in Figure 1 for high and low angle regions.

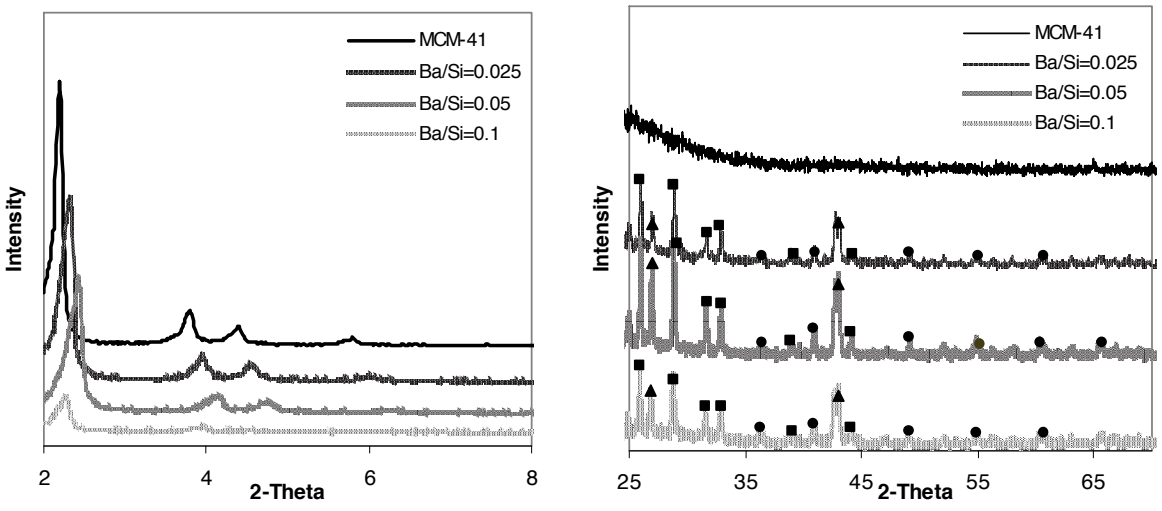

Figure 1. XRD patterns of MCM-41 and Ba/ MCM-41 (▲; BaO and BaO_2, ■; $BaSi_2O_5$ and Ba_2SiO_4, ●; $Ba(NO_3)_2$).

MCM-41 is known to exhibit a well-ordered lattice structure with hexagonal unit cell. The reflections obtained in the low angle region are known to be characteristic of the MCM-41 structure. X-ray diffraction results exhibit 3 well-resolved diffractions, due to the ordered hexagonal array of parallel silica tubes, which correspond to the reflections of (100), (110), and (200) planes. Occasionally a fourth diffraction peak with a notably lower intensity may be observed for (210) reflection. XRD patterns of bare MCM-41 synthesized

by direct hydrothermal route showed (100), (110), (200), and (210) reflections at 2θ of 2.24, 3.88, 4.46, and 5.85, which are consistent with the literature.[4] By increasing the Ba/Si molar ratio the peak intensities were decreased, also the peaks at 2θ of 2.24, 3.88, and 4.46 were shifted to the wider diffraction angle, which may be due to the incorporation of barium atoms into the mesostructure, decreasing the space of the lattice structure (d100). The peaks at 2θ of 26.03, 28.84, 32.79, 33.04, 38.88, and 44.7 degrees were obtained in high angle XRD patterns, attributed to the formation of barium silicates ($BaSi_2O_5$, Ba_2SiO_4).[24] The peaks at 2θ of 36.71, 48.9, and 55.45 degrees were attributed to barium nitrate ($Ba(NO_3)_2$) and the peaks at 2θ of 27.8, 42.6, and 57.9 degrees were attributed to the presence of barium oxides.[24,25]

The textural properties and the lattice parameters of samples were measured by BET (N_2 adsorption-desorption) and the results are summarized together with X-ray diffraction analyses in the Table. The characteristic lattice parameter (the repeating distance "a" between 2 pore centers) was calculated from Eq. (3):[23]

$$a = 2d_{(100)}/\sqrt{3} \tag{3}$$

The pore wall thickness δ was then estimated from the average pore diameter (d_p) and the lattice parameter (a) using Eq. (4):[23]

$$\delta = a - 0.95d_p \tag{4}$$

The average pore diameters of the bare MCM-41 and Ba/MCM-41 (Ba/Si; 0.025-0.1) were determined as 3.0 nm, 2.7 nm, 2.5 nm, and 2.8 nm, respectively. The pore volume decreased significantly with the incorporation of Ba into the silica, which indicates pore filling. In addition, the lattice parameters and pore wall thicknesses were estimated as 1.1 and 1.9 for bare and Ba/MCM-41, respectively. However, the pore wall thicknesses were increased by the incorporation of Ba. The nitrogen adsorption-desorption isotherms and BJH pore size distributions are given in Figure 2. The BET isotherms of the synthesized materials exhibited a Type IV isotherm and monodispersed pore size distributions were obtained. The BET surfaces were significantly

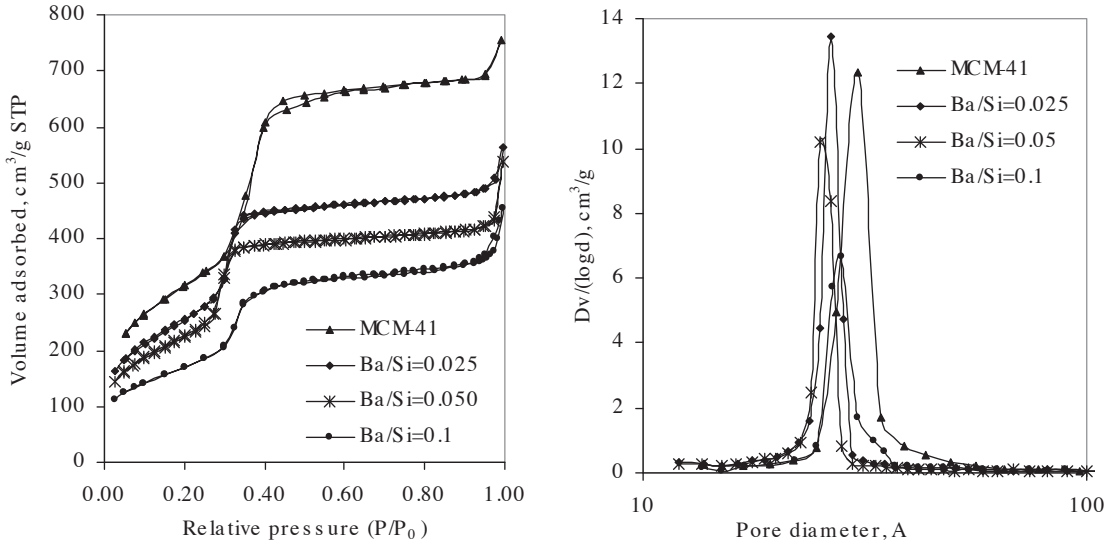

Figure 2. Nitrogen adsorption-desorption isotherms and BJH pore size distributions of pure MCM-41 and Ba/MCM-41.

decreased from 1156 to 722 m^2/g with incorporation of Ba (Ba/Si: 0.1). The increase in pore diameter indicated adsorption of Ba metal into the pores, enlarging the pore structure, which had been observed as shifts in XRD analysis in the low angle region (Figure 1). As a result the increase in pore size was thought to occur as a result of metal clustering.

A TGA-DTA curve of Ba/MCM-41 before calcination is shown in Figure 3. A similar weight loss pattern was observed for bare MCM-41. Thermogravimetric weight change recorded under air atmosphere showed significant weight loss (∼58%) due to removal of surfactant in a temperature range of 200-350 °C. The weight loss was stabilized at 550 °C, which was determined as the calcination temperature for this study.

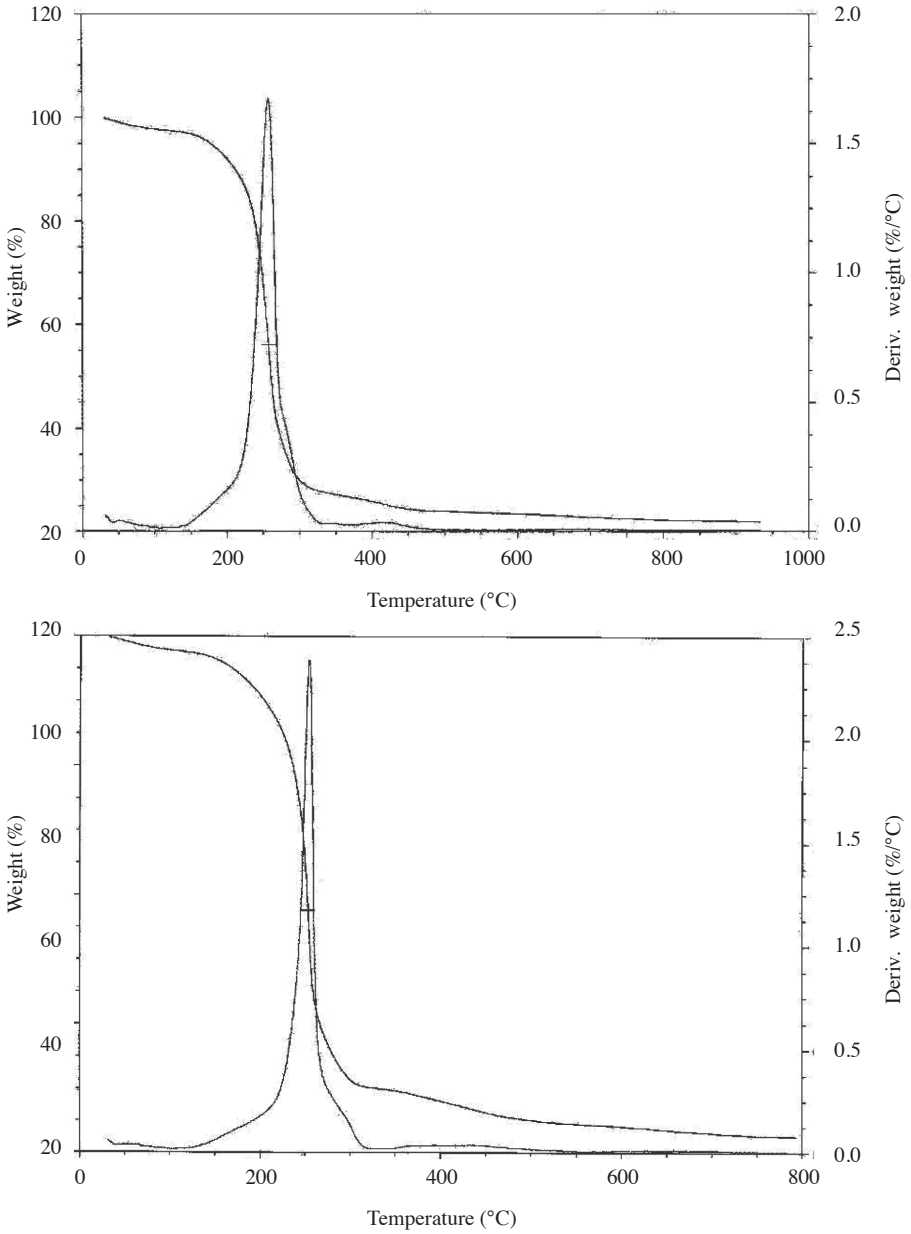

Figure 3. (a) TGA-DTA curves of pure MCM-41., (b)TGA-DTA curves of Ba/MCM-41 (Ba/Si: 01).

Table. Physical properties of pure MCM-41 and Ba/MCM-41.

Sample	d(100)	Lattice parameter "a" (nm)	Surface area (BET) (m^2/g)	Pore volume (cm^3/g)	Av.pore diameter 'd_p" (nm)	Pore wall thickness "δ"
MCM-41	3.94	4.55	1156	0.9	3.0	1.1
Ba-MCM-41 Ba/Si: 0.025	3.80	4.39	931	0.6	2.7	1.8
Ba-MCM-41 Ba/Si: 0.05	3.62	4.18	913	0.4	2.5	1.8
Ba-MCM-41 Ba/Si: 0.1	3.83	4.42	722	0.4	2.8	1.9

FT-IR spectra of MCM-41 and Ba/MCM-41 with a molar ratio of Ba/Si: 0.1 are shown in Figure 4. The band at 3450 cm^{-1} is attributed to the stretching mode of adsorbed water. The peak at 3746 cm^{-1} is ascribed to the fundamental stretching vibrations of the terminal Si–OH group.[26] The disappearance of the stated peak implied condensation of water, which was reflected as a decrease in Si–OH groups. The 2 bands observed at 1082 and 1228 cm^{-1} belonged to internal and external asymmetric Si-O stretching modes.[27] The spectrum obtained at 1636 cm^{-1} was characteristic of SiO_2.[28] The main feature is the spectrum obtained at 1430 cm^{-1}, which was attributed to Ba species.[29,30]

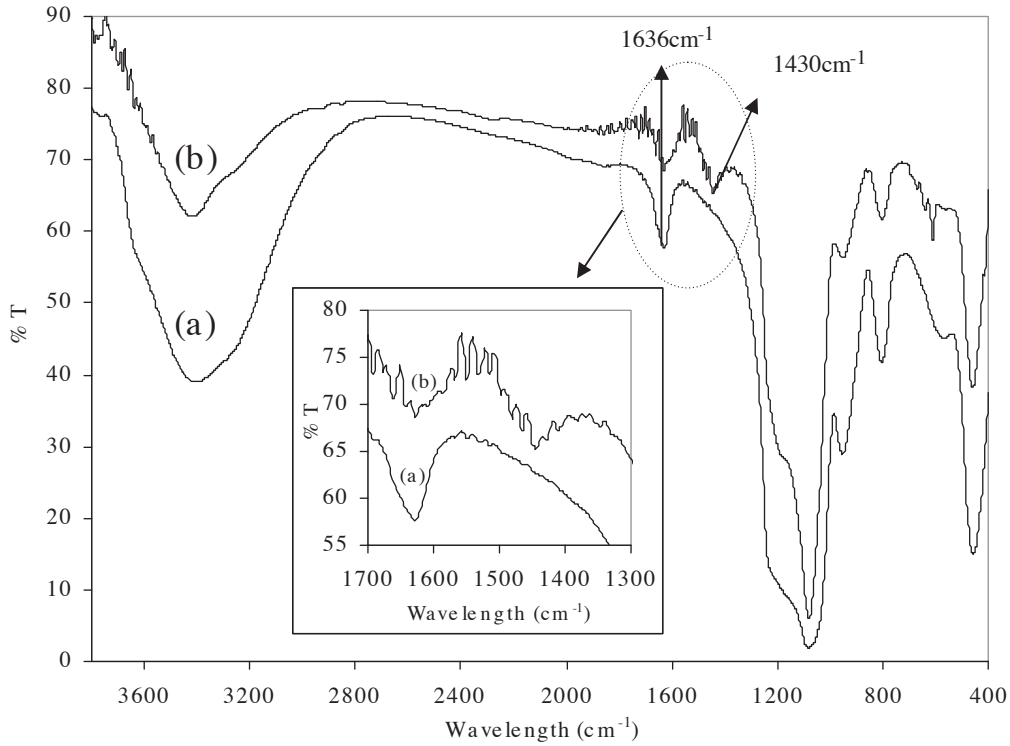

Figure 4. FT-IR spectra of (a) pure MCM-41 and (b) Ba/MCM-41 (Ba/Si: 01).

The SEM image and EDS map of Ba/MCM-41 with a molar ratio of Ba/Si: 0.1 is shown in Figure 5. EDS maps exhibited the distribution of species (O, Si, Ba) on the surface of the material. Metal clustering with an XRD pattern and pore diameter could clearly be seen in EDS maps. Homogeneous pore size distribution for Ba/Si molar ratio < 0.1 was obtained (Figure 2), indicating a monodispersed structure.

The TEM images of pure MCM-41 and Ba/MCM-41 with a molar ratio of Ba/Si: 0.1 (Figure 6) show that the mesoporous structure is preserved.

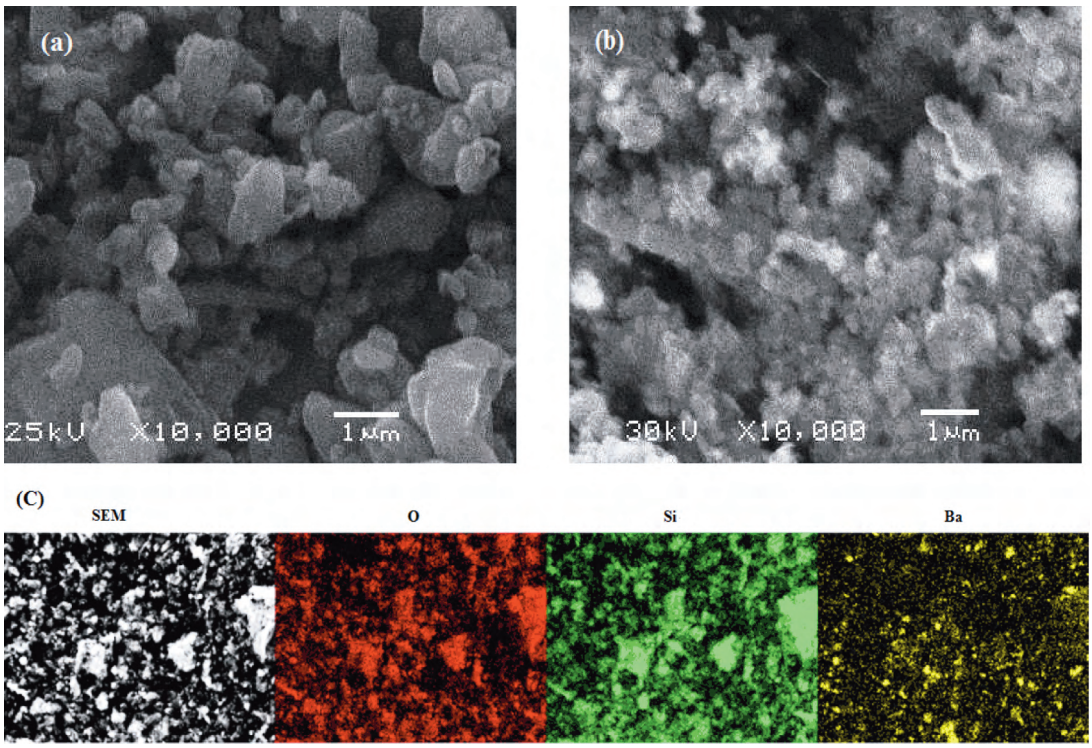

Figure 5. SEM images of (a) MCM-41 (b) Ba/ MCM-41(Ba/Si; 0.1) and (c) EDS maps of Ba/MCM-41(Ba/Si: 0.1).

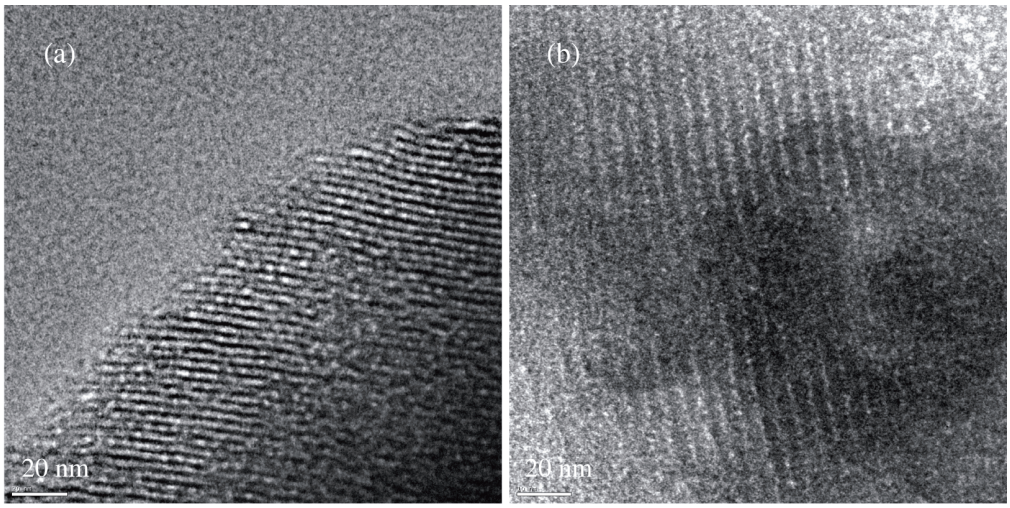

Figure 6. TEM images of (a) MCM-41 (b) Ba/ MCM-41(Ba/Si: 0.1).

In the present study, Ba/MCM-41 materials with high surface areas were synthesized for different Ba/Si molar ratios. Direct hydrothermal synthesis was applied. Characterization studies were performed to clarify the effect of metal addition on molecular structure. The preparation technique applied in this study was thought to enhance uniform dispersion of the metal throughout the structure. Prior to our investigations there was no information in the literature about Ba containing MCM-41 catalysts or synthesis of these catalysts via direct hydrothermal route. Comparison of catalysts synthesized by various supports attracts synthesis of Ba/MCM-41 due to its high surface area, pore structure, and uniform Ba dispersion.

Conclusions

Ba/MCM-41 samples with high Ba/Si molar ratios were synthesized by direct hydrothermal route. The formation of barium oxides and barium silicates was evidenced by XRD measurements. These materials were shown to have rather narrow pore size distributions and high surface areas, with average pore diameter of 3 nm. The SEM image of Ba/MCM-41 with a molar ratio of Ba/Si: 0.1 exhibits distorted hexagonal morphology. Ba/MCM-41 synthesized with molar ratios smaller than 0.1 preserved its crystal structure as implied by the results of low angle XRD patterns. The decrease in surface areas for Ba/Si indicated coverage of pores. Metal clustering was observed for Ba/Si: 0.1 molar ratio, which was implied by BET measurements and clarified by SEM-EDS maps. Treatment of N_2 adsorption-desorption data with BJH isotherm revealed a monodispersed structure. FT-IR spectra of Ba/MCM-41 showed bands at 1430 cm^{-1}, which belong to Ba metal, implying a good attachment of the metal throughout the surface. The characterization results stated above indicated the synthesis of a uniformly dispersed metal adsorbed MCM-41, which was concluded to have potential uses in NOx adsorption studies.

Acknowledgements

Financial support from University Research Funds through Gazi University (06/2007-20 and 06/2007-54) is gratefully acknowledged.

References

1. Kresge, C. T.; Leonowicz, M. E.; Roth, W. J.; Vartuli, J. C.; Beck, J. S. *Nature* **1992**, *359,* 710.
2. Beck, J. S.; Vartuli, J. C.; Roth, W. J.; Leonowicz, M. E.; Kresge, C. T.; Schmitt, K. D.; Chu, C. T. W.; Olsen, D. H.; Sheppard, E. W.; McCullen, S. B.; Higgins, J. B.; Schlenker, J. L. *J. Am. Chem. Soc.* **1992**, *114*, 10834-10843.
3. Shin, M. Y.; Nam, C. M.; Park, D. W.; Chang, J. S. *Appl. Catal. A: General* **2001,** *211*, 213.
4. Lensveld, D. *On the preparation and characterisation of MCM-41 supported heterogeneous nickel and molybdenum catalysts,* Ponsen & Looijen BV, 2003, 7-25.
5. Zhang, Q.; Wang, Y.; Ohishi, Y.; Shishido, T.; Takehira, K. *J. Catal.* **2001,** *202,* 308.
6. Wang, X. X.; Lefebvre, F.; Patarin, J.; Basset, J.M. *Microporous and Mesoporous Mater.* **2001,** *42,* 269-276.
7. Li, Z.; Gao, L.; *J. Physics and Chemistry of Solids* **2003**, *64*, 223-228.

8. Øye, G.; Sjöblom, J.; Stöcker, M. *Advances in Colloid and Interface Sci.* **2001,** *89-90*, 439-466.
9. Taguchi, A.; Schüth, F. *Microporous and Mesoporous Mater.* **2005***, 77*, 1-45.
10. Gomes, H. T.; Selvam, P.; Dapurkar, S. E.; Figueiredo, J. L.; Faria, J. L. *Microporous and Mesoporous Mater.* **2005***, 86,* 287-294.
11. Vizcaíno, A. J.; Carrero, A.; Calles, J. A. *Int. J. Hydrogen Energy* **2007,** *32,* 1450.
12. Makshina, E. V.; Nesterenko, N. S.; Siffert, S.; Zhilinskaya, E. A.; Aboukais A.; Romanovsky, B. V. *Catal. Today* **2008,** *131*, 427.
13. Vetrivel S.; Pandurangan, A. *J. Molecular Catal. A: Chemical* **2006***, 246*, 223.
14. Wan, Y.; Ma, J.; Wang, Z.; Zhou, W.; Kaliaguine, S. *Appl. Catal. B: Environmental* **2005***, 59*, 235-242.
15. Liu, C. C.; Teng, H. *Appl. Catal. B: Environmental* **2005***, 58,* 69-77.
16. Bhargava, S. K.; Akolelar, D. B. *J. Colloid and Interface Sci.* **2005***, 281*, 171-178.
17. Oktar, N., Mitome, J.; Holmgreen, E. M.; Ozkan, U. S. *J. Molecular Catal. A: Chemical* **2006***, 259,* 171-182.
18. Fridell, E.; Skoglundh, M.; Westerberg, B.; Johansson, S.; Smedler, G. *J. Catal.* **1999,** *183,* 196-209.
19. Cant, N. W.; Patterson, M. J. *Catal. Today* **2002***, 73*, 271-278.
20. Poulston S., Rajaram, R. R. *Catal. Today* **2003***, 81,* 603-610.
21. Pisarello, M. L.; Milt, V.; Peralta, M. A.; Querini, C. A.; Miro, E. E. *Catal. Today* **2002***, 75***,** 465-470.
22. Laurent, F.; Pope, C. J.; Mahzoul H.; Delfosse, L.; Gilot, P.; *Chem. Eng. Sci.* **2003,** *58,* 1793-1803.
23. Sener, C.; Dogu, T.; Dogu, G. *Microporous and Mesoporous Mater.* **2006***, 94,* 89-98.
24. Li, Q.; Brown, S. E.; Broadbelt, L. J.; Zheng, J-G.; Wu, N. Q. *Microporous and Mesoporous Mater.* **2003***, 59,* 105-111.
25. Downs, B.; Swaminathan, R.; Bartelmehs, K. *Amer. Mineral.* **1993***, 78,* 1104-1107.
26. Selvarej, M.; Pandurangan, A.; Seshadri, K. S. *Appl. Catal. A: General* **2003***, 242,* 347.
27. Bhowera, S. S.; Singh, A. P. *J. Molecular Cat. A: Chemical* **2007***, 266,* 118-130.
28. Castro, F. L.; Santos, J. G.; Fernandes, G. J. T.; Araújo, A. S.; Fernandes, V. J.; Politi, M. J.; Brochsztain, S. *Microporous and Mesoporous Mater.* **2007***, 102,* 258-264.
29. Tsay, J. D.; Fang, T. T.; Gubiotti, T. A.; Ying, J. Y. *J. Mater. Sci.* **1998***, 33,* 3721.
30. Coutures, J. P.; Odier, P.; Proust, C. *J. Mater. Sci.* **1992***, 27,* 1849.